JOURNAL OF THE AMERICAN COLLEGE OF CARDIOLOGY
© 2015 BY THE AMERICAN COLLEGE OF CARDIOLOGY FOUNDATION
PUBLISHED BY ELSEVIER INC.

VOL. 66, NO. 23, 2015
ISSN 0735-1097/$36.00
http://dx.doi.org/10.1016/j.jacc.2015.09.094

Idiopathic Ventricular Arrhythmias Originating From the Pulmonary Sinus Cusp

Prevalence, Electrocardiographic/Electrophysiological Characteristics, and Catheter Ablation

Zili Liao, MD,* Xianzhang Zhan, MD,* Shulin Wu, MD,* Yumei Xue, MD,* Xianhong Fang, MD,* Hongtao Liao, MD,* Hai Deng, MD,* Yuanhong Liang, MD,* Wei Wei, MD,* Yang Liu, MD,* Feifan Ouyang, MD†

ABSTRACT

BACKGROUND Idiopathic ventricular arrhythmias (VAs) originating from the pulmonary sinus cusp (PSC) have not been sufficiently clarified.

OBJECTIVES The goal of this study was to investigate the prevalence, electrocardiographic characteristics, mapping, and ablation of idiopathic VAs arising from the PSC.

METHODS Data were analyzed from 218 patients undergoing successful endocardial ablation of idiopathic VAs with a left bundle branch block morphology and inferior axis deviation.

RESULTS Twenty-four patients had VAs originating from the PSC. In the first 7 patients, initial ablation performed in the right ventricular outflow tract failed to abolish the clinical VAs but produced a small change in the QRS morphology in 3 patients. In all 24 patients, the earliest activation was eventually identified in the PSC, at which a sharp potential was observed preceding the QRS complex onset by 28.2 ± 2.9 ms. The successful ablation site was in the right cusp (RC) in 10 patients (42%), the left cusp (LC) in 8 (33%), and the anterior cusp (AC) in 6 (25%). Electrocardiographic analysis showed that RC-VAs had significantly larger R-wave amplitude in lead I and a smaller aVL/aVR ratio of Q-wave amplitude compared with AC-VAs and LC-VAs, respectively. The R-wave amplitude in inferior leads was smaller in VAs localized in the RC than in the LC but did not differ between VAs from the AC and LC.

CONCLUSIONS VAs arising from the PSC are not uncommon, and RC-VAs have unique electrocardiographic characteristics. These VAs can be successfully ablated within the PSC. (J Am Coll Cardiol 2015;66:2633–44)

The right ventricular outflow tract (RVOT) and left ventricular outflow tract are the most common sites of origin for idiopathic ventricular tachycardia (VT) or premature ventricular contractions (PVCs) absent overt structural heart disease (1-6). Less commonly, idiopathic ventricular arrhythmias (VAs) can originate from the pulmonary artery (PA) (7-10). Histopathological studies have shown that ventricular myocardium may extend into the aorta and PA beyond the semilunar valves (11-13). Thus, by extending into the great vessels with abnormal automaticity or triggered activity, the ventricular myocardium may be the underlying mechanism of these VAs (8). VAs originating from the aortic root may be ablated within the aortic sinus cusp (ASC) or from the right/left coronary cusp commissure (2,14,15). However, most PA-VAs are located >10 mm above the pulmonary valve (PV)

Listen to this manuscript's audio summary by *JACC* Editor-in-Chief Dr. Valentin Fuster.

From the *Department of Cardiology, Guangdong Cardiovascular Institute, Guangdong General Hospital, Guangdong Academy of Medical Sciences, Guangdong, China; and the †Department of Cardiology, Asklepios Klinik St. Georg, Hamburg, Germany. The authors have reported that they have no relationships relevant to the contents of this paper to disclose. Drs. Z. Liao and Zhan contributed equally to this work.

Manuscript received July 14, 2015; revised manuscript received September 23, 2015, accepted September 24, 2015.

ABBREVIATIONS AND ACRONYMS

AC = anterior cusp
ASC = aortic sinus cusp
ECG = electrocardiogram
LBBB = left bundle branch block
LC = left cusp
PA = pulmonary artery
PSC = pulmonary sinus cusp
PV = pulmonary valve
PVC = premature ventricular contraction
RC = right cusp
RF = radiofrequency
RFCA = radiofrequency catheter ablation
RV = right ventricle
RVOT = right ventricular outflow tract
SR = sinus rhythm
VA = ventricular arrhythmia
VT = ventricular tachycardia

and could be successfully ablated in the PA (9,10). Given that little is known about the characteristics of VAs originating from the pulmonary sinus cusp (PSC) (9,16), the goal of the present study was to evaluate the prevalence, electrocardiographic characteristics, mapping, and ablation of idiopathic VAs arising from the PSC.

SEE PAGE 2645

METHODS

Between August 2012 and August 2014, a total of 244 patients (148 men; age 56.1 ± 14.5 years) underwent endocardial radiofrequency catheter ablation (RFCA) at Guangdong General Hospital for idiopathic VAs with a left bundle branch block (LBBB) morphology and inferior axis deviation. In 26 patients, the arrhythmia could not be eliminated because of latent serious radiofrequency (RF)-related complications, indeterminate site of earliest ventricular activation, or inability to stabilize the ablation catheter during the procedure. In the remaining 218 patients, the successful ablation site was located on the endocardial RVOT (n = 148), in the ASC (n = 46), or within the PSC (n = 24). The present study consisted of the latter 24 patients. When the QRS morphology of clinical VAs was tested with an electrocardiogram (ECG) algorithm to determine VA origin, all idiopathic VAs were identified as arising from the RVOT (2-10,17). In addition, no patients had any overt structural heart disease on echocardiography. The study was approved by the institutional review board of Guangdong General Hospital.

ECG AND ELECTROPHYSIOLOGICAL ANALYSES. Detailed analysis of clinical PVC/VAs was performed offline by using an electrophysiological data acquisition system with a recording speed of 50 to 100 mm/s or 12-lead ECG with a recording speed of 25 to 50 mm/s. During clinical VAs, QRS morphology on leads I, II, III, aVR, and aVL was assessed, as well as: 1) R-wave amplitude in leads I, II, III, aVF, V_1, and V_2 and the III/II R ratio; 2) duration of R-wave complex in leads II, III, and aVF; 3) Q-wave amplitude in leads aVR and aVL and the QS aVR/aVL ratio; and 4) the precordial R/S transitional zone. In addition, the precordial R-wave transitional zone was analyzed during sinus rhythm (SR). All measurements were independently performed by 3 physicians.

After providing written informed consent, and after withdrawal of antiarrhythmic drugs for a duration of >5 half-lives, all patients underwent an electrophysiological evaluation. Catheters were placed into the heart under fluoroscopy through the femoral vessels. If clinical arrhythmias failed to occur spontaneously, programmed stimulation was performed. The protocol consisted of ventricular stimulation at 2 basic drive cycle lengths with <2 extra stimuli to a minimum coupling interval of 230 ms. If VA was not inducible at baseline, intravenous isoproterenol infusion (2 to 5 μg/min) was administered to provoke clinical arrhythmias.

MAPPING AND RFCA. In patients with frequent PVCs or short-run VT, 3-dimensional electroanatomical mapping was used, as reported previously (18). In brief, mapping was performed using a steerable 7.5-F, D-curve catheter with a 3.5-mm irrigated-tip electrode (NaviStar ThermoCool, Biosense Webster, Diamond Bar, California). If necessary, the mapping catheter was advanced via an SR0 long sheath introduced through the right femoral vein to the right ventricle. Point-by-point mapping was performed to create anatomic maps, and activation mapping was used to identify the origin during PVCs or VT in the study. Pace mapping was also performed, with the lowest pacing output (2 to 20 mA) and pulse width (0.5 to 10 ms), to capture the ventricular myocardium at the site of earliest activation. A suitable target for ablation was selected based on the earliest activation times during the arrhythmia.

In the initial 7 patients, mapping began in the RVOT. If suitable ablation sites were not found, the PA and left ventricular outflow tract were mapped. In the subsequent 17 patients, 3-dimensional mapping was initially performed in the RVOT and subsequently in the PA before ablation. Right ventriculography and/or pulmonary arteriography were also performed to locate the position of the PV (**Figure 1**) and to mark the pulmonary annulus on 3-dimensional mapping (**Figures 2, 3, and 4**). Detailed mapping in the PSC was achieved by using a reversed U curve of the ablation catheter, which can facilitate the stability of a mapping catheter within the PSC. Importantly, an 8.5-F long sheath was always used and advanced into the right ventricle to allow for a reversed U curve in the PA. The long sheath can stabilize the mapping catheter and help rotate it clockwise or counterclockwise to access 3 individual PSCs. Left ventricular access was achieved via a retrograde aortic and/or transseptal approach. For left-sided procedures, unfractionated heparin was administered to maintain activated clotting times between 250 and 300 s.

Irrigated RF current was delivered in power-controlled mode, with a maximum power of 40 W,

FIGURE 1 PSC Anatomy

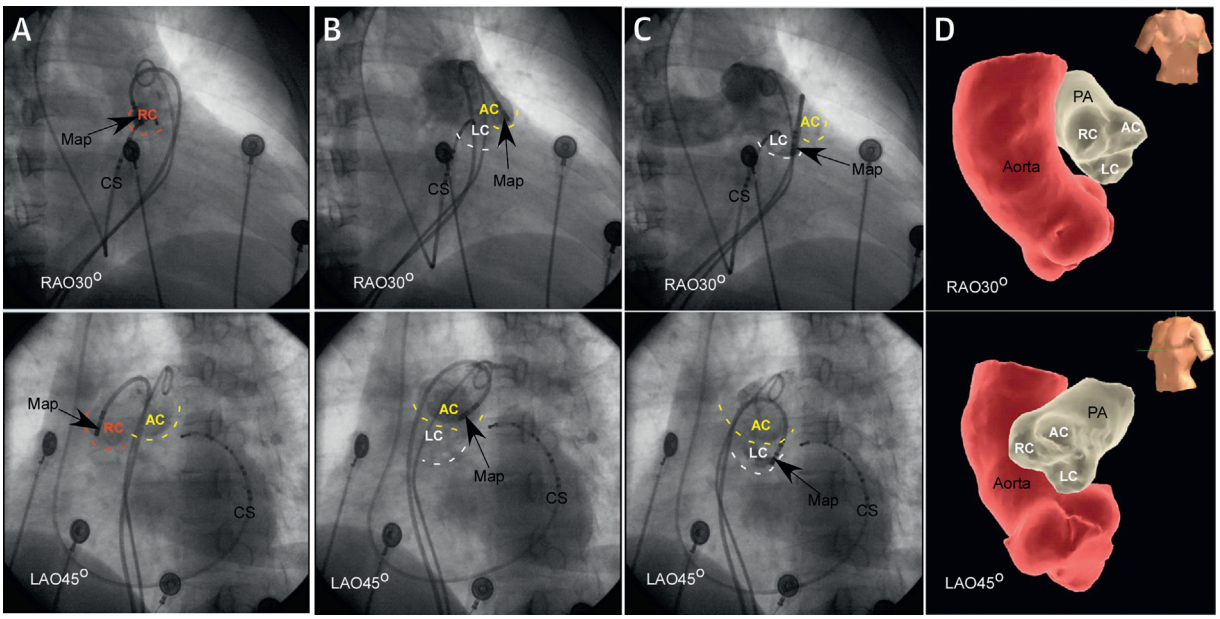

The right (30°) oblique view **(upper)** and the left (45°) oblique view **(lower)** show the left, anterior, and right pulmonary sinus cusp (PSC) via **(A to C)** PA angiography and **(D)** 3-dimensional computer tomography images. Note the 3 PSCs are not at the same level: the left cusp (LC) is situated at the lowest, the anterior and right pulmonary cusp situated relatively superiorly. AC = anterior cusp; CS = coronary sinus; Map = mapping catheter; PA= pulmonary artery; RC = right cusp.

a temperature limit of 43°C, and a flow rate of 20 ml/min. During RF delivery, if a decreased frequency/elimination of VAs occurred within the initial 15 s, the application was maintained and carefully titrated for 60 s. Ventriculography, PA angiography, or coronary angiography was performed to determine the precise location of the ablation catheter positioned at the successful application site. After successful ablation, intravenous administration of isoproterenol and programmed stimulation were performed to reinitiate clinical VAs.

Acute success was defined as either absence of spontaneous or provoked clinical VAs at the end of the procedure or absence of the latter on 24-h ECG monitoring post-ablation off antiarrhythmic drugs. Antiarrhythmic drugs were not reinitiated if ablation was acutely successful. Each patient returned for evaluation in the hospital's outpatient arrhythmia center at 2 weeks, 1 month, and every 3 months thereafter. Transthoracic echocardiography and 24-h Holter monitoring were performed the day after the procedure and at the 3-month follow-up visit.

STATISTICAL ANALYSIS. Continuous variables are expressed as mean ± SD, and categorical variables as numbers and percentages. The Student *t* test and Fisher exact test were used for comparisons of the continuous variables and categorical variables between the 2 groups, respectively. A p value <0.05 was considered significant.

RESULTS

Patient and clinical data are shown in **Table 1**. Previous ablation had been performed in 7 of the 24 patients (1 ablation attempt in 5 patients and 2 attempts in 2 patients). Two of the 7 patients had failed ablation procedures; RFCA resulted in acute success in the remaining 5 patients. However, VAs with the same morphologies recurred during follow-up in these patients. Neither ventriculography nor intracardiac echocardiography was used to evaluate catheter position. VA burden on 24-h Holter ECG is shown in **Table 1**.

ECG AND ELECTROPHYSIOLOGICAL CHARACTERISTICS

The surface ECG during either VT or PVCs exhibited a typical LBBB morphology with an inferior axis in all patients (**Figure 5**, Online Figure 1). Before ablation, a small difference in QRS morphology existed in 2 of 24 patients; 1 was frequently observed, the other less frequently. The subtle differences in QRS morphology were mainly in the R-wave in inferior leads. The remaining 22 (92%) had single QRS morphologies.

FIGURE 2 Fluoroscopy and Mapping in Patient #6

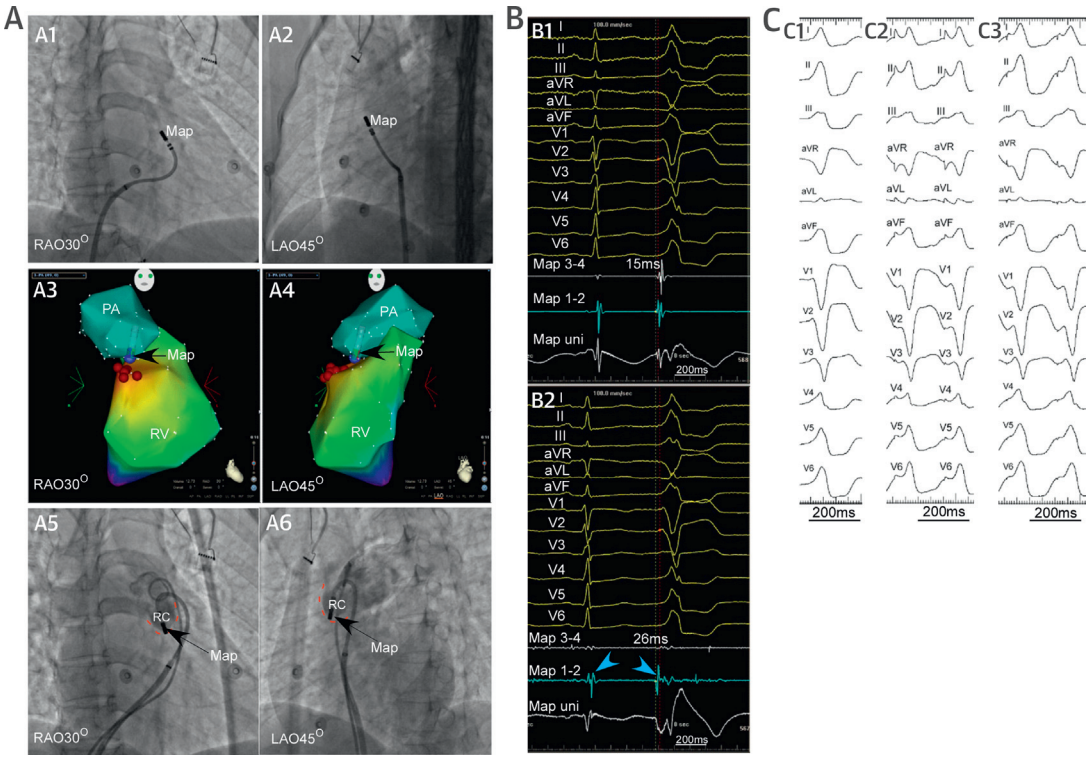

(A1) Right (30°) and **(A2)** left (45°) oblique radiographic views of the Map at the unsuccessful ablation site at the right ventricular outflow tract (RVOT) free wall just below the RC. **(A3)** Right (30°) and **(A4)** left (45°) oblique electroanatomical maps of the same male patient demonstrate the earliest activation at the free wall RVOT **(red)**, the unsuccessful ablation point **(red tag)**, and anatomical mapping of the pulmonary artery with the mapping catheter just within the RC **(blue tag)**. **(A5)** Right (30°) and **(A6)** left (45°) oblique radiographic views of the Map at the successful ablation site within the RC, demonstrated by pulmonary artery angiography with a 6-F pigtail. **(B1)** Surface electrocardiographic (ECG) leads and intracardiac recordings from a Map at the site of earliest ventricular activation within the RVOT. Note that the earliest activation precedes QRS by 15 ms with an RS morphology in unipolar recording. **(B2)** Surface ECG leads and intracardiac recordings from a Map at the site of earliest ventricular activation within the RC. Note that the local late sharp component **(blue arrows)** follows a low-amplitude potential during sinus rhythm **(blue arrows)**. This potential preceded QRS onset by 26 ms during the premature ventricular contraction (PVC) with simultaneous activation in bipolar and unipolar activation and QS morphology in unipolar recording. Twelve-lead QRS morphology during **(C1)** spontaneous PVCs, pacing at the sites of earliest activation at the **(C2)** RVOT free wall, and at the **(C3)** RC. Note that that QRS morphology was only perfectly matched when pacing at the RC, although QRS morphology during pacing at the RVOT free wall was very similar to that during clinical PVC. RV = right ventricle; other abbreviations as in Figure 1.

Frequent PVCs or short runs of VT occurred spontaneously in 20 patients. Isoproterenol infusion was administered to provoke the frequent VAs in the other 4 patients. Clinical VAs were not inducible by programmed ventricular stimulation in any patients.

In the RVOT, the earliest activation was at the posteroseptal region in 3, the mid-septal in 3, the anteroseptal in 3, the middle free wall in 3, the anterolateral in 6, and the posterolateral region in 6 (Figure 2). The local ventricular activation preceded the onset of the QRS complex by 19.9 ± 3.3 ms, and a good pace map (10 of 12 leads matched in QRS morphology in 3 patients and 11 of 12 leads matched in 5 patients) was obtained at the site of earliest ventricular activation in 8 patients (33%). No presystolic or late diastolic potentials were recorded. The mean distance from the site of earliest ventricular activation in the RVOT to the closest PSC portion was 4.1 ± 2.6 mm.

In the initial 7 patients with RVOT ablation, RFCA resulted in transient suppression of VAs in 4 patients. However, additional RF energy deliveries in the RVOT could not abolish the VAs in any patient. After initial ablation in the RVOT, a small change in the QRS morphology developed in 3 patients; there was no

FIGURE 3 Fluoroscopy and Mapping in Patient #16: VAs From LC

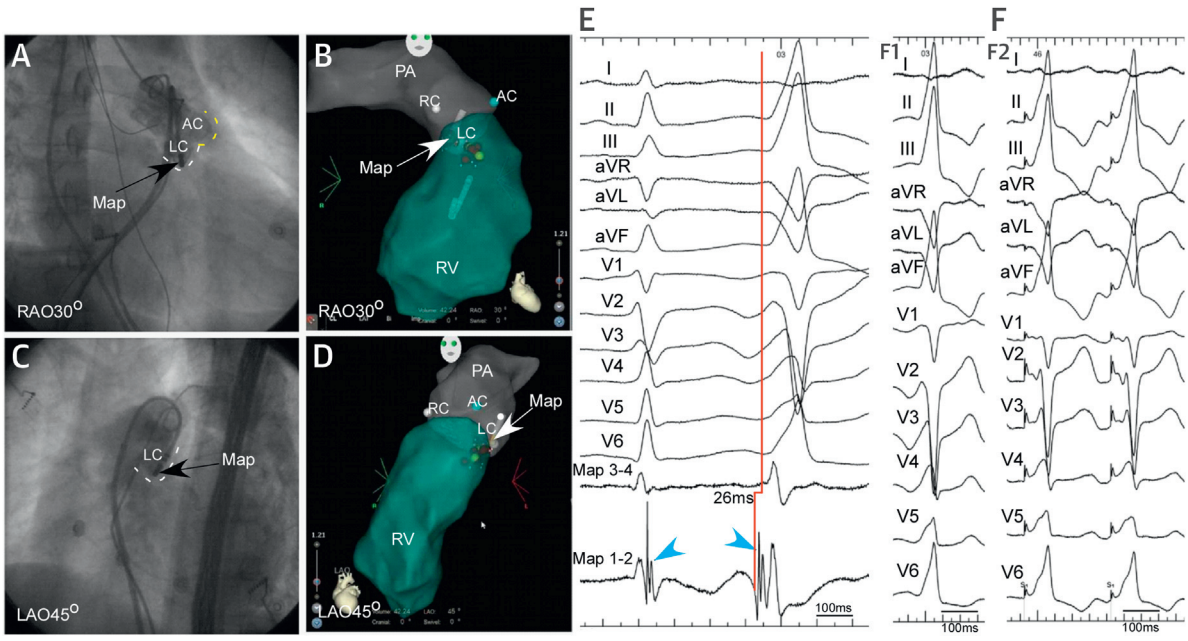

(A) Right (30°) and **(C)** left (45°) oblique radiographic views of the Map at the successful ablation site within the LC. **(B)** Right (30°) and **(D)** left (45°) oblique electroanatomical maps of the same patient demonstrate the successful ablation site within the LC. **(E)** Surface ECG leads and intracardiac recordings from a Map at the site of earliest ventricular activation within the AC. Fractionated potentials with a sharp potential **(blue arrowheads)** were recorded during sinus rhythm and the sharp potential preceded QRS onset by 26 ms during the PVC at the successful ablation site. **(F1)** Spontaneous PVC and **(F2)** paced-QRS morphology during pace mapping. Paced-QRS morphology at the site of earliest activation does not match that of spontaneous QRS in I, V_1, and V_2. Abbreviations as in Figures 1 and 2.

evidence of subtle changes in QRS morphology before ablation in these 3 patients (Figure 6).

When mapping in the pulmonary root, a 2-component (near-field and far-field) activation was observed at the site of earliest ventricular activation during SR in all 24 patients (Figures 2, 3, and 4). During VAs, the reversal relationship of the near-field ventricular signal and the far-field signal was noted, and no isolated presystolic potentials were observed at that site in any patient. On bipolar recording, the earliest ventricular activation was identified in the PSC. The ventricular activation on unipolar recording demonstrated QS morphology with almost simultaneous activation and the earliest discrete potential on bipolar recording (Figures 2 and 4). Pace mapping was obtained in all 24 patients (mean lowest pacing output 7.5 ± 2.4 mA), but a good pace map was achieved in 20 patients only (83%). Of these 20 patients, paced ECG morphology matched the clinical VA in 12 of 12 leads in 1 patient (Figure 2), in 11 of 12 leads in 9 patients, and in 10 of 12 leads in 10 patients (Figure 3). The major differences between the spontaneous and paced QRS were in leads V_1 and V_2 (31%), similar to pacing in RVOT.

The final successful ablation site was in the right cusp (RC) in 10 patients (42%), the left cusp (LC) in 8 (33%), and the anterior cusp (AC) in the remaining 6 (25%). Of these 24 successful RF sites, 22 were at the bottom of the PSC; the remaining 2 (both LC-VAs) were located 4 mm and 4.5 mm beyond the PSC bottom, respectively. The targeted potential at the final ablation site preceded QRS complex onset of clinical VAs by 28.2 ± 2.9 ms, significantly greater than the earliest activation time recorded in the RVOT ($p < 0.05$). The number of RF lesions ranged from 5 to 15 (mean 8.3 ± 3.6) in the series of 24 patients (13.3 ± 1.8 in the initial 7 patients vs. 6.2 ± 1.4 in the last 17 patients; $p < 0.05$). Procedural time and fluoroscopic time were 124.9 ± 18.1 min and 5.3 ± 1.8 min, respectively. After successful ablation in the PSC, a discrete potential at the late phase of the QRS complex during SR was still recorded in all 24 patients.

COMPARING ECG AND ELECTROPHYSIOLOGICAL PARAMETERS FOR PSC VAs. The results of the ECG parameters of these VAs with their determined origins are given in Table 2. There were no significant

FIGURE 4 Fluoroscopy and Mapping in Patient #24: VAs Originating From Pulmonary AC

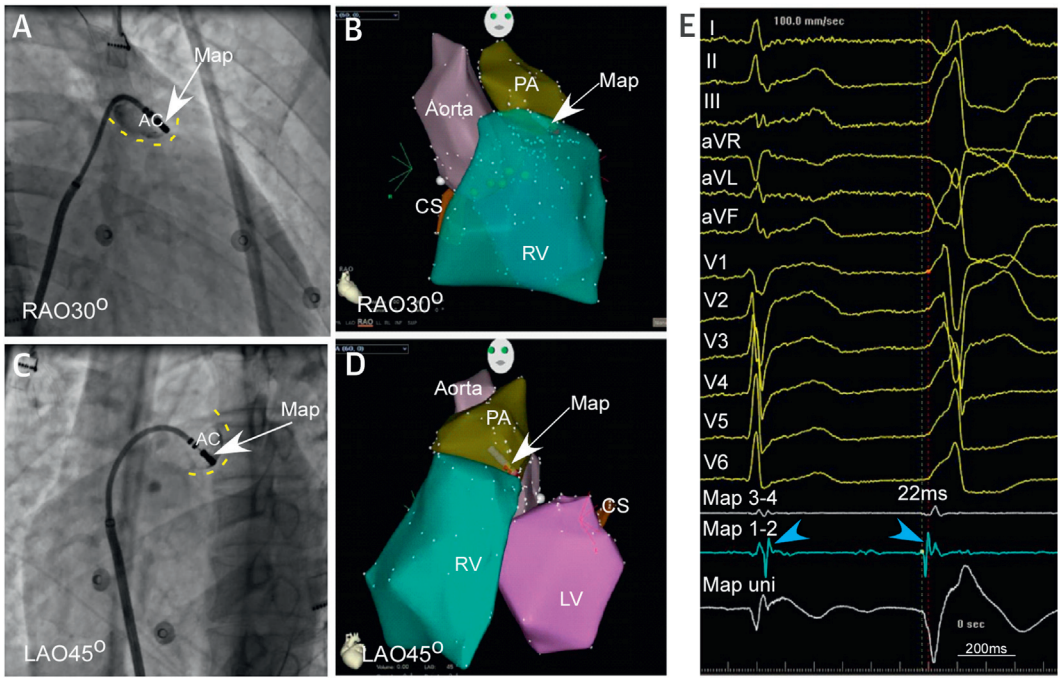

(A) Right (30°) and **(C)** left (45°) oblique radiographic views of the mapping catheter with reversed U curve at the successful ablation site within the AC. **(B)** Right (30°) and **(D)** left (45°) oblique electroanatomical maps of the same patient demonstrate the successful ablation point within the AC. **(E)** Surface ECG leads and intracardiac recordings from a Map at the site of earliest ventricular activation within the AC. Two components were recorded, with the larger near-field component **(blue arrows)** following the smaller far-field component at the site of earliest activation; also, the earliest activation precedes the QRS by 22 ms with a reversed relationship of both components during PVCs compared with these components during sinus rhythm. Abbreviations as in Figures 1 and 2.

TABLE 1 Patient Characteristics (N = 24)

Age, yrs	36 ± 11
Male	6
Duration of symptoms, months	34 ± 37
Clinical VAs	
Only PVCs	20
PVCs, nonsustained VT	4
PVCs, nonsustained/sustained VT	0
VA burden on 24-h Holter ECG (beats)	
Before ablation	27,384 ± 12,236
At 1 day post-ablation	0
At 3 months post-ablation	88 ± 70
Structural heart disease	0
LVEF (%) before ablation	62.8 ± 5.6
Antiarrhythmic drugs	2.3 ± 0.6
Previously failed ablation	7

Values are mean ± SD or n.

ECG = electrocardiogram; LVEF = left ventricular ejection fraction; PVCs = premature ventricular contractions; VA = ventricular arrhythmia; VT = ventricular tachycardia.

differences in the clinical characteristics. In comparing lead I polarity, QRS morphology exhibited a large R-wave in 10 RC-VAs, 1 AC-VA, and 2 LC-VAs (Table 2, Figure 5, Online Figure 1). The R-wave amplitude in lead I was significantly higher in the RC-VAs than in the AC-VAs and LC-VAs but did not differ between VAs from the AC and LC.

There was a notch on the R-wave in the inferior leads in 11 patients; the origin was located at the RC in 7 patients, at the AC in 2 patients, and at the LC in 2 patients. The R-wave amplitude in the inferior leads (the ratio of the R-wave amplitude in lead III/II) was significantly smaller in the RC-VAs than in the AC-VAs and LC-VAs. The QRS duration was longer in the RC-VAs than in both the AC-VAs and LC-VAs. A QS-wave was presented in aVR in all 24 patients and in aVL in 23 patients except 1 patient with RC-VAs. The transitional zone was often observed at V_4, occurring from V_3 in 2 of 10 RC-VAs, 2 of 6 AC-VAs, and 1 of 8 LC-VAs.

There were no differences between local ventricular activation time relative to the QRS onset,

FIGURE 5 ECGs With VAs

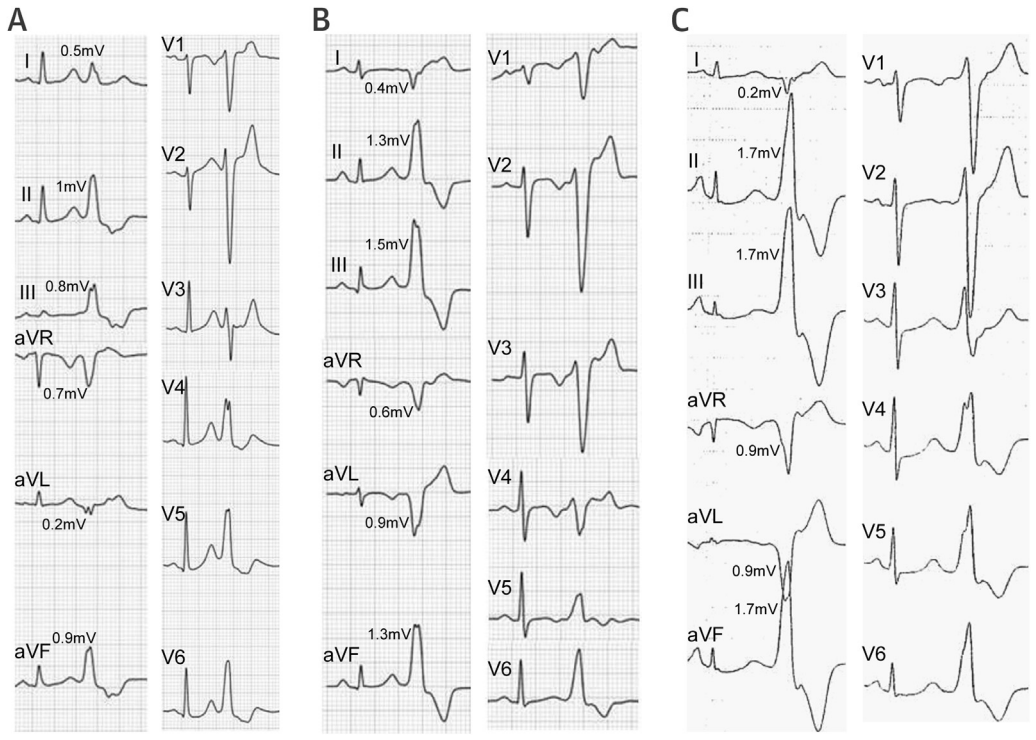

These ECG recordings are from **(A)** a 58-year-old female, in whom the ventricular arrhythmia (VA) origin was located at the RC, with 2 previous failed ablation attempts in the RVOT; **(B)** a 31-year-old female with VAs originating from the AC; and **(C)** a 29-year-old female with VAs originating from the LC. Abbreviations as in Figures 1 and 2.

RF duration, and number of RF applications among the origin sites within the 3 PSCs. A sharp potential was recorded in all patients. Low-amplitude and broad atrial potentials were observed only in VAs with left atrial origin (4 of 8). A relatively low-output pacing was achieved in all patients.

No procedure-related complications occurred in any of the 24 patients, and no PV damage was found according to echocardiographic results. All patients were free of arrhythmias, without antiarrhythmic drugs, during a follow-up period of 9 ± 3 months. Post-ablation VA burden on 24-h Holter ECG is shown in Table 1.

DISCUSSION

The pulmonary root is the distal part of the RVOT that supports the 3 semilunar leaflets of the PV. There are 3 distinct junctions or rings that can be appreciated in the region (11–13). The semilunar valvular leaflets have distal attachment at the sinotubular junction, which separates the PSCs from the tubular component of the pulmonary trunk. The PSC wall is supported throughout its circumference by the muscular right ventricular (RV) infundibulum, where the 2 join across the anatomic ventriculoarterial junction. At the base, the semilunar attachments of the leaflets cross the anatomic ventriculoarterial junction, creating a third ring (i.e., the hemodynamic ventriculoarterial junction). The interdigitation of the semilunar attachments with the 3 rings presents a crown-like configuration. However, the 3 PSCs are not at the same level: the LC is situated at the lowest level, with the AC and RC situated relatively superior (Figure 1).

The RV musculature could extend at the base of the pulmonary root and, in a sleeve-like manner, more distally into the PA between the cusps and into the valve tissue itself. Hasdemir et al. (12) reported that in 17% of autopsied hearts, myocardium extending beyond the ventriculoarterial junction was present. Another autopsy study showed that the prevalence of such myocardium extensions was even higher, up to 74% (13). Nevertheless, these results were obtained

FIGURE 6 QRS Morphological Changes Pre-ablation and Post-ablation

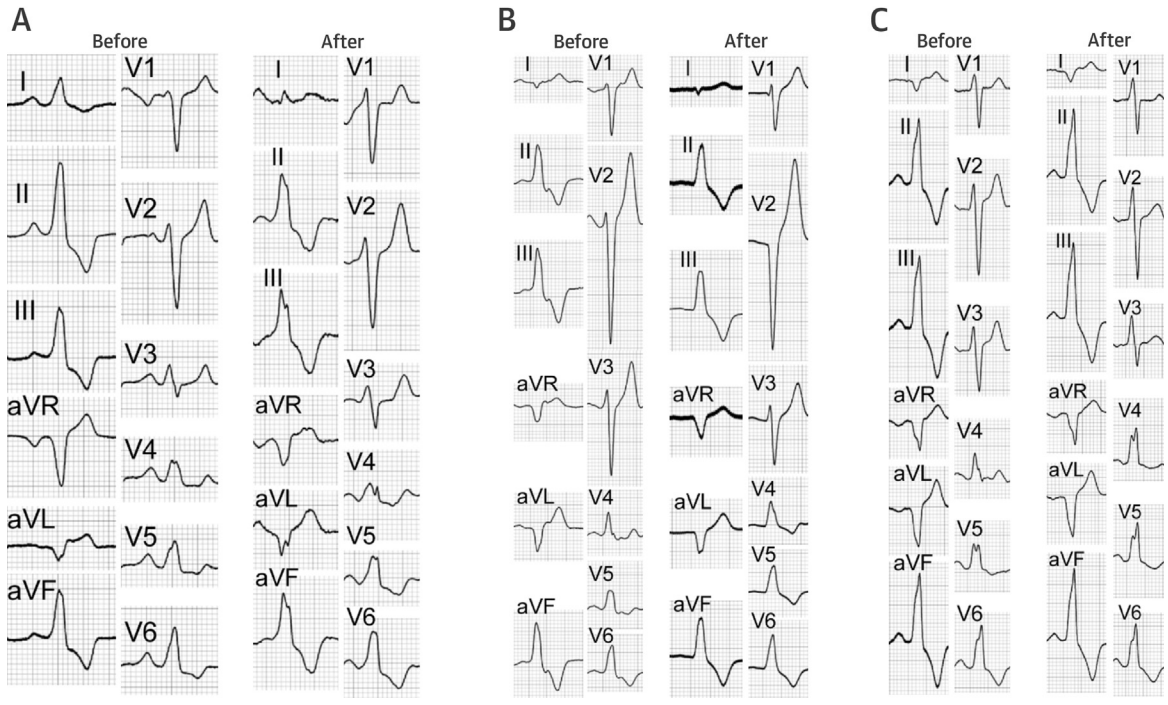

(A) ECG recordings before and after the initial unsuccessful ablation at the RVOT from **(A)** a 26-year-old female, in whom the VA origin was located within the RC, with 2 previous failed ablation attempts in the RVOT; **(B)** a 42-year-old female with VAs originating from the AC; and **(C)** a 47-year-old female with VAs originating from the LC. Abbreviations as in Figures 1, 2, and 5.

from subjects in whom the majority had no clinical VAs. Recently, by using voltage mapping and intracardiac echocardiography, Liu et al. (19) speculated that the myocardial extension beyond the PV existed in 92% of control patients and 88% of patients with RVOT arrhythmia. The presence of fibrosis and fatty tissue among these muscular sleeves may create a possible VA substrate for PSC-VAs (12).

PREVALENCE OF PSC-VAs. Several studies have reported the prevalence of VAs arising from PA, and among the RVOT arrhythmia foci, 21% to 46% were localized beyond the PV (9,19). Most of these VAs were located 8 mm above the PV. Only some cases had the successful ablation site located closely above the PV (8,16). However, the distance between the successful ablation site and bottom of the cusp of the PV has not been described in detail. In the present study, by using pulmonary arteriography and/or ventriculography, VAs with a PSC location were noted in 24 (11%) of 218 idiopathic outflow tract-like VAs treated by using RFCA (**Central Illustration**). The low incidence of PSC-VAs reported in previous studies may be due mainly to unawareness of ablation in the PSC without angiography or intracardiac echocardiography, especially for LC-VAs. Less commonly, standard ventriculography may not accurately reflect the relationship of the catheter position to the valve. In addition, small sample sizes could account for the low prevalence of PSC-VAs in previous reports. Conversely, the high incidence of PSA-VAs in our study may be an overestimation in real practice because most of these subjects were admitted to our center for complex arrhythmia ablation or for previously failed ablation elsewhere. Furthermore, the VAs were not induced by programmed stimulation in any patient, strongly suggesting a mechanism most likely due to automaticity from the myocardium with the PSC.

MAPPING AND RFCA WITHIN PSC. It has been reported that VAs can be successfully ablated in the PA (8-10,19). Similar to interruption conduction in an atrioventricular accessory pathway, PA-VAs could theoretically be successfully abolished by targeting the origin in the PA, the preferential conduction pathway, or the insertion into the RVOT. However, the proximal portion of the myocardial extension and

its attachment with RV myocardium may be wide and bifurcated, resembling the breakthrough from the myocardial sleeves with the pulmonary veins (10,20). During arrhythmia, activation originating from the PSC would have conducted to the RVOT through the myocardial extensions and could lead to a change in QRS morphology due to the conduction block over the myocardial extension's breakthrough and conduction property. In addition, this special anatomic structure may be responsible for detouring the activation impulse during RF delivery in the RVOT, as observed in 3 patients. Consequently, most of the successful ablation sites were at the distal and narrow portions of the myocardial extension or at the PA-VAs origin.

Discrete potentials noted within the great artery, representing myocardial extensions into the PA, were useful in guiding ablation of PA-VAs (8,10,16). In the present study, all VAs were successfully ablated in the PSC. The ablation target was only identified by the earliest ventricular activation, which preceded the QRS onset by 28.2 ± 2.9 ms with simultaneous activation in bipolar and unipolar recordings. The local electrograms at the successful site in the PSC-VAs in these 24 patients differ from those in VAs from ASC, which present with the earliest activation as isolated presystolic potentials and a mismatched timing in bipolar and unipolar recordings in most patients with VA from the left coronary sinus cusp (2,4–6). In all 24 patients, 2 components at the earliest activation site during VAs were demonstrated, and the first potential during VAs was recorded after the ventricular electrograms during SR before and after ablation. Pace mapping could be performed at the earliest activation site in all patients without high output; a good pace map was obtained at that site in 20 patients. However, no discrete potential was recorded in any patient at the earliest activation site in the RVOT, and initial ablation there failed to abolish the clinical VAs in the first 7 patients but resulted in small QRS morphological changes. Furthermore, mapping at the PSC can be facilitated with a reversed U curve, which was always supported with a long sheath in the right ventricle.

However, the high number of irrigated RF applications and the relatively short activation time of local electrogram-to-QRS onset of 28.2 ± 2.9 ms in our series was different from mapping and ablation results of VA from the ASC. This phenomenon may be explained by several factors: 1) it has a clear learning curve, and it remains challenging to position D-curve catheter tips with a reversed U curve in the PSC; 2) precise catheter tip movement in individual PSCs was sometimes difficult by clockwise/counterclockwise-rotated manipulation of the mapping catheter, which may lead to some tiny areas inaccessible in the PSC; and 3) while mapping and ablation found that the VAs were located at the PSC nadir in most of our patients, the origin from RVOT close to the PSC cannot be totally excluded in some patients (although irrigated RF energy at RVOT failed to abolish VAs in our initial 7 patients). Based on these results, we speculate that the arrhythmogenic foci in the present study may be within or near the PSC (13). During VAs, conduction propagates through preferential conduction pathways and exits from the distal RVOT.

TABLE 2 ECG Characteristics During VAs

	Right Cusp (n = 10)	Anterior Cusp (n = 6)	Left Cusp (n = 8)
R-wave amplitude in I, mV	0.37 ± 0.17*	−0.30 ± 0.31	−0.03 ± 0.29
R-wave amplitude in II, mV	1.29 ± 0.20	1.56 ± 0.46	1.98 ± 0.42
R-wave amplitude in III, mV	1.04 ± 0.28*	1.74 ± 0.34	1.98 ± 0.35
R-wave amplitude III/II	0.80 ± 0.16*	1.16 ± 0.23	1.00 ± 0.09
Q-wave amplitude in aVR, mV	0.79 ± 0.12	0.79 ± 0.33	1.06 ± 0.28
Q-wave amplitude in aVL, mV	0.48 ± 0.18*	0.97 ± 0.18	1.11 ± 0.33
Q-wave amplitude aVL/aVR	0.63 ± 0.29*	1.37 ± 0.43	1.07 ± 0.32
R-wave amplitude in aVF, mV	1.14 ± 0.25*	1.62 ± 0.42	2.11 ± 0.45
R-wave amplitude in V_1, mV	0.16 ± 0.07	0.32 ± 0.28	0.26 ± 0.09
S-wave amplitude in V_1, mV	1.47 ± 0.43	1.17 ± 0.48	1.58 ± 0.65
R/S ratio on V1	0.11 ± 0.03	0.28 ± 0.20	0.19 ± 0.10
R-wave amplitude in V_2, mV	0.34 ± 0.17	0.50 ± 0.29	0.48 ± 0.23
S-wave amplitude in V_2, mV	2.17 ± 0.92	2.22 ± 0.80	2.53 ± 0.74
R/S ratio on V_2	0.16 ± 0.06	0.28 ± 0.25	0.20 ± 0.08
Incidence of large R in I	10 (100)*	1 (17)	2 (25)
Incidence of notching in II, III, and aVF	7 (70)	2 (33)	2 (25)
Duration of QRS, ms	155 ± 15.2*	134.2 ± 14.0	133.8 ± 12.5

Values are mean ± SD or n (%). *$p < 0.05$.
Abbreviations as in Table 1.

Catheter ablation within the PSC carries the potential risk of PA stenosis and damage to the left main coronary artery (21,22). However, these complications were not reported in previous studies or in our study. This outcome may be due mostly to the larger vessel and more connective tissue compared with the pulmonary veins (11). In addition, better contact with effective energy delivery within the PSC by curving the ablation catheter to form a reversed U curve may be another potential factor. Accordingly, careful attention should be paid to power and impedance characteristics to avoid steam pop during RF delivery.

ECG FINDINGS. Several studies have attempted to describe ECG criteria to identify the successful ablation site in the PA. Sekiguchi et al. (9) reported that the R-wave amplitude in the inferior ECG leads, the aVL/aVR ratio of the Q-wave amplitude, and the R/S ratio in lead V_2 were statistically larger in PA-VAs than in RVOT-VAs. Other previous reports demonstrated no such specific ECG findings for

CENTRAL ILLUSTRATION **VAs Originating From the PSC**

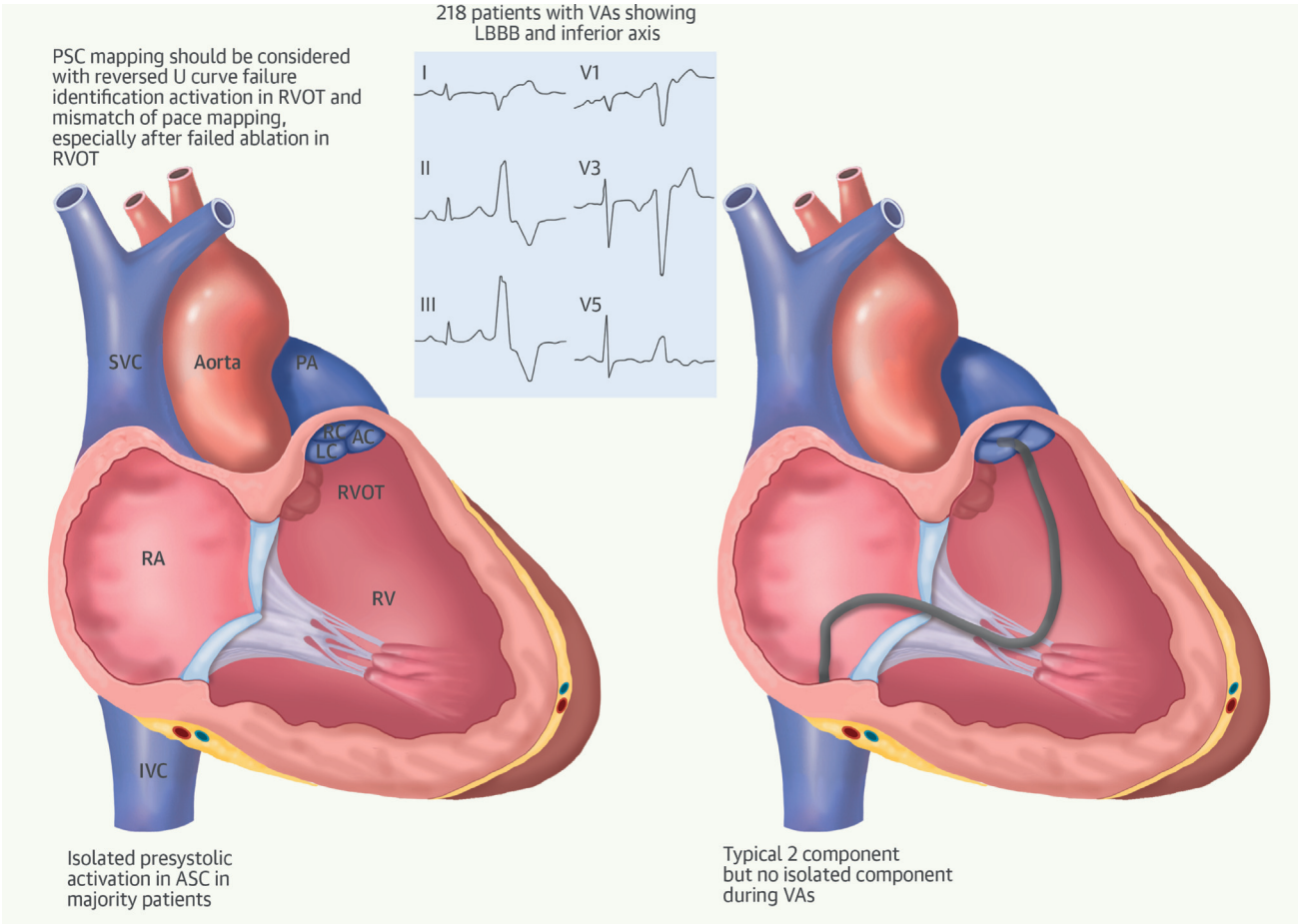

Liao, Z. et al. J Am Coll Cardiol. 2015; 66(23):2633–44.

In 218 patients with ventricular arrhythmias (VAs) showing left bundle branch block (LBBB) morphology and inferior axis deviation, 24 had VAs originating from the pulmonary sinus cusp (PSC). Mapping of PSC should be considered with a reversed U curve after failed identification of the earliest activation in the right ventricular outflow tract (RVOT) and mismatch of pace mapping, especially in failed ablation in RVOT. In addition, a surface electrocardiogram in I and III/II ratio can differentiate the VAs with right cusp (RC) origin from left cusp (LC)/anterior cusp (AC). IVC = inferior vena cava; PA = pulmonary artery; RA = right atrium; RV = right ventricle; SVC = superior vena cava.

PA-VAs (8,10). The discrepancy might be explained because, in the study by Sekiguchi et al., 92% of PA-VAs were located in the LC, which is located most superiorly in the right ventricle and more leftward and more anteriorly, eventually resulting in higher inferior lead R-wave amplitudes, a larger aVL/aVR ratio of Q-wave amplitude, and a larger R/S ratio in lead V_2. In our study, all patients with LC-VAs had high inferior lead R-wave amplitudes, which is consistent with the findings of Sekiguchi et al. For the VAs with RC origin, the R-wave amplitudes were significantly smaller than those with LC-VAs but did not differ from the AC-VAs, except for lead II. The QRS duration was longer in the RC-VAs than in the AC-VAs and LC-VAs. In addition, QRS features (e.g., a small III/II ratio, the higher incidence of notch in the inferior leads) were similar to that in VAs below the pulmonary cusp (23). In addition, a recent study reported that VAs arising from the PV region had a relatively smaller R-wave (0.14 ± 0.16 mV) in lead I (24). The detailed location of peripulmonic valve VAs was not mentioned in their report. In the present study, a large R-wave in lead I was frequently observed in the RC-VAs; the R-wave amplitude

(0.37 ± 0.17 mV) was significantly larger than in AC-VAs (-0.30 ± 0.31 mV) and LC-VAs (-0.03 ± 0.29 mV). These findings can be explained by the phased excitation from the RVOT free wall to the left ventricle in RC-VAs, during which the total QRS duration could be prolonged and the absolute R-wave magnitude decreased (25).

STUDY LIMITATIONS. Because of product unavailability in China, intracardiac echocardiography was not used to identify catheter location. Instead, pulmonary arteriography and/or ventriculography was performed to determine the PV position and the relationship of the successful ablation site in the PA and the PV cusp. In addition, the distance measurement according to 3-dimensional mapping provided the best estimation in this study. Second, there was no evidence of structural abnormality on echocardiography and abnormal voltage and activation on 3-dimensional mapping during SR in these 24 patients. Diagnosis of RV cardiomyopathy is unlikely, although occult fibrosis may not be totally excluded without cardiac magnetic resonance imaging. Finally, comparison of ECG characteristics between the RVOT-VA and PSC-VA was not performed; further investigation is needed to determine whether some ECG characteristics can differentiate both VAs.

CONCLUSIONS

In patients with VA demonstrating LBBB morphology and inferior axis deviation, mapping in the RVOT may not identify the site of earliest activation and/or mismatched QRS morphology by pace mapping. In such patients with failed ablation, mapping at the PSC should be performed, as VAs arising from the PSC are not uncommon, and RC-VAs have unique ECG characteristics. These VAs can be successfully ablated with a reversed U curve within the PSC.

ACKNOWLEDGMENT The authors thank Dr. Michael Shehata for his assistance.

REPRINT REQUESTS AND CORRESPONDENCE: Dr. Shulin Wu, Department of Cardiology, Guangdong Cardiovascular Institute, Guangdong General Hospital, Zhongshan Road #106, Yuexiu District, Guangzhou 510080, Guangdong, China. E-mail: shulin_gdgh@163.com.

PERSPECTIVES

COMPETENCY IN PATIENT CARE AND PROCEDURAL SKILLS: In patients with VA that exhibit LBBB and inferior axis morphology, pace mapping in the RVOT may not identify the site of earliest activation or generate mismatched QRS morphology. In such patients, particularly when ablation has failed, mapping at the PSC should be performed to identify VAs that can be successfully ablated.

TRANSLATIONAL OUTLOOK: Larger studies are needed to determine the prevalence of VA arising from the PSC and establish the long-term efficacy of ablation at this site.

REFERENCES

1. Callans DJ, Menz V, Schwartzman D, et al. Repetitive monomorphic tachycardia from the left ventricular outflow tract: electrocardiographic patterns consistent with a left ventricular site of origin. Am J Cardiol 1997;29:1023–7.

2. Ouyang F, Fotuhi P, Ho SY, et al. Repetitive monomorphic ventricular tachycardia originating from the aortic sinus cusp: electrocardiographic characterization for guiding catheter ablation. J Am Coll Cardiol 2002;39:500–8.

3. Ventura R, Steven D, Klemm HU, et al. Decennial follow-up in patients with recurrent tachycardia originating from the right ventricular outflow tract: electrophysiologic characteristics and response to treatment. Eur Heart J 2007;28:2338–45.

4. Kamakura S, Shimizu W, Matsuo K, et al. Localization of optimal ablation site of idiopathic ventricular tachycardia from right and left ventricular outflow tract by body surface ECG. Circulation 1998;98:1525–33.

5. Yamada T, Litovsky SH, Kay GN. The left ventricular ostium: an anatomic concept relevant to idiopathic ventricular arrhythmias. Circ Arrhythm Electrophysiol 2008;1:396–404.

6. Tada H, Nogami A, Naito S, et al. Left ventricular epicardial outflow tract tachycardia: a new distinct subgroup of outflow tract tachycardia. Jpn Circ J 2001;65:723–30.

7. Timmermans C, Rodriguez LM, Medeiros A, et al. Radiofrequency catheter ablation of idiopathic ventricular tachycardia originating in the main stem of the pulmonary artery. J Cardiovasc Electrophysiol 2002;13:281–4.

8. Timmermans C, Rodriguez LM, Crijns HJ, et al. Idiopathic left bundle-branch block-shaped ventricular tachycardia may originate above the pulmonary valve. Circulation 2003;108:1960–7.

9. Sekiguchi Y, Aonuma K, Takahashi A, et al. Electrocardiographic and electrophysiologic characteristics of ventricular tachycardia originating within the pulmonary artery. J Am Coll Cardiol 2005;45:887–95.

10. Tada H, Tadokoro K, Miyaji K, et al. Idiopathic ventricular arrhythmias arising from the pulmonary artery: prevalence, characteristics, and topography of the arrhythmia origin. Heart Rhythm 2008;5:419–26.

11. Anderson RH, Razavi R, Taylor AM. Cardiac anatomy revisited. J Anat 2004;205:159–77.

12. Hasdemir C, Aktas S, Govsa F, et al. Demonstration of ventricular myocardial extensions into the pulmonary artery and aorta beyond the ventriculo-arterial junction. Pacing Clin Electrophysiol 2007;30:534–9.

13. Gami AS, Noheria A, Lachman N, et al. Anatomical correlates relevant to ablation above the semilunar valves for the cardiac electrophysiologist: a study of 603 hearts. J Interv Card Electrophysiol 2011;30:5–15.

14. Yamada T, McElderry HT, Doppalapudi H, et al. Idiopathic ventricular arrhythmias originating from the aortic root prevalence, electrocardiographic and electrophysiologic characteristics, and results of radiofrequency catheter ablation. J Am Coll Cardiol 2008;52:139–47.

15. Bala R, Garcia FC, Hutchinson MD, et al. Electrocardiographic and electrophysiologic features of ventricular arrhythmias originating from the right/left coronary cusp commissure. Heart Rhythm 2010;7:312–22.

16. Srivathsan KS, Bunch TJ, Asirvatham SJ, et al. Mechanisms and utility of discrete great arterial potentials in the ablation of outflow tract ventricular arrhythmias. Circ Arrhythm Electrophysiol 2008;1:30–8.

17. Yoshida N, Inden Y, Uchikawa T, et al. Novel transitional zone index allows more accurate differentiation between idiopathic right ventricular outflow tract and aortic sinus cusp ventricular arrhythmias. Heart Rhythm 2011;8:349–56.

18. Ouyang F, Cappato R, Ernst S, et al. Electroanatomic substrate of idiopathic left ventricular tachycardia: unidirectional block and macroreentry within the purkinje network. Circulation 2002;105:462–9.

19. Liu CF, Cheung JW, Thomas G, et al. Ubiquitous myocardial extensions into the pulmonary artery demonstrated by integrated intracardiac echocardiography and electroanatomic mapping: changing the paradigm of idiopathic right ventricular outflow tract arrhythmias. Circ Arrhythm Electrophysiol 2014;7:691–700.

20. Saito T, Waki K, Becker AE. Left atrial myocardial extension onto pulmonary veins in humans: anatomic observations relevant for atrial arrhythmias. J Cardiovasc Electrophysiol 2000;11:888–94.

21. Vaseghi M, Cesario DA, Mahajan A, et al. Catheter ablation of right ventricular outflow tract tachycardia: value of defining coronary anatomy. J Cardiovasc Electrophysiol 2006;17:632–7.

22. Walsh KA, Fahy GJ. Anatomy of the left main coronary artery of particular relevance to ablation of left atrial and outflow tract arrhythmias. Heart Rhythm 2014;11:2231–8.

23. Dixit S, Gerstenfeld EP, Callans DJ, et al. Electrocardiographic patterns of superior right ventricular outflow tract tachycardias: distinguishing septal and free-wall sites of origin. J Cardiovasc Electrophysiol 2003;14:1–7.

24. Ebrille E, Chandra VM, Syed F, et al. Distinguishing ventricular arrhythmia originating from the right coronary cusp, peripulmonic valve area, and the right ventricular outflow tract: utility of lead I. J Cardiovasc Electrophysiol 2014;25:404–10.

25. Tada H, Ito S, Naito S, et al. Prevalence and electrocardiographic characteristics of idiopathic ventricular arrhythmia originating in the free wall of the right ventricular outflow tract. Circ J 2004;68:909–14.

KEY WORDS mapping, pulmonary, radiofrequency, tachycardia

APPENDIX For a supplemental figure, please see the online version of this article.